

Wideband Waveguide Polarizer Development for SETI

P. Lee and P. Stanton

Ground Antennas and Facilities Engineering Section

A wideband polarizer for the Deep Space Network (DSN) 34-meter beam-waveguide antenna is needed for the Search for Extraterrestrial Intelligence (SETI) project. The results of a computer analysis of a wideband polarizer are presented in this article.

I. Introduction

The Search for Extraterrestrial Intelligence (SETI) sky survey will scan a frequency range from 1 to 10 GHz, using the Deep Space Network (DSN) 34-meter beam-waveguide antennas. To minimize the number of feeds that accommodate this broad frequency range, wideband components are necessary. In [1], a design for a wideband quarter-wave polarizer was presented. The polarizer consists of a rectangular waveguide with all four walls loaded with natural or artificial dielectrics. This article describes the performance of such a polarizer, as analyzed with Hewlett-Packard's 85180A High-Frequency Structure Simulator (HFSS), a software package that uses the finite-element method to analyze closed structures.

II. Method

Figure 1 shows the geometry of the polarizer. An incident TE_{10} mode excites a quasi- TE_{10} mode in the loaded waveguide. An incident TE_{01} mode excites a quasi- TE_{01} mode, which has a different propagation constant from the quasi- TE_{10} mode. As the two modes travel through the

loaded waveguide, the phase shift between them is proportional to the difference between the propagation constants. Since the propagation constants are functions of frequency, the phase shift is also. It was found in [1] that by loading the four walls of the polarizer with dielectric, the differential phase shift can be held constant to within a given tolerance over a wider bandwidth than in polarizers where only two opposing walls are loaded.

The design parameters were chosen by assuming that the forms of the quasi- TE_{10} and quasi- TE_{01} modes in the loaded waveguide did not vary much from the TE_{10} and TE_{01} modes in an unloaded waveguide. Since the fields of the TE_{10} and TE_{01} modes are zero on the sidewalls parallel to the E-field components, and since the dielectric on the walls is thin, only the dielectric on the walls perpendicular to the E-field was considered when each mode was analyzed for the initial design. This simpler problem of a waveguide with only two walls loaded has been solved [2].

The polarizer was analyzed on a Sun SPARC 1+ workstation using HFSS software, revision A.01.00. The workstation has approximately 500 MB of hard-disk memory

available in the user partition. The HFSS software analyzes arbitrary closed structures with finite-element methods. It computes the eigenmodes at each port by using the number of modes chosen by the user. Then the S-parameters for the structure are calculated to within a tolerance set by the user. The finite-element mesh is refined over a number of passes until the desired tolerance is achieved. Once a mesh is created at one frequency, the same mesh can be used in a sweep over nearby frequencies. After HFSS calculates the S-parameters, it calculates the impedances at each port.

The first step in analyzing the polarizer was to determine the propagation constants of the quasi- TE_{10} and quasi- TE_{01} modes in the loaded waveguide. A 0.25-in. long slice of the waveguide was used. Electric and magnetic planes of symmetry were employed to reduce the cross-section to one quarter of its original size. By placing the planes of symmetry as shown in Fig. 2(a), the mode resulting from an incident TE_{10} mode could be analyzed. Similarly, Fig. 2(b) shows the placement of the planes of symmetry used to analyze the mode resulting from an incident TE_{01} mode. An adaptive pass was run at 11.0 GHz to create the finite-element mesh, and then a frequency sweep was performed from 6.0 GHz to 16.0 GHz in 0.5-GHz intervals. Adaptive passes were later run at the endpoint frequencies to check the validity of the mesh. The frequency range was chosen for measurement convenience and will be scaled to the SETI frequency range later.

The polarizer could not be analyzed as one structure because this presented too large a problem for the memory in the workstation. An interface section consisting of a thin slice of the loaded waveguide and a thin slice of empty waveguide, as shown in Fig. 3(a), was analyzed instead. The HFSS software assumes that each port is connected to an infinitely long structure having the same cross-section as the port, so the effects of the interface by itself can be deduced from this structure. The S-parameters for this structure were calculated over the frequency range 9.5 GHz to 15.5 GHz. HFSS has the capability of computing the S-parameters resulting from the addition of an extension to any port if the extension has the same cross-sectional geometry as the port. By using this feature, the S-parameters for the structure shown in Fig. 3(b) were computed. Finally, the S-parameters from the structures shown in Figs. 3(a) and 3(b) were combined to create the S-parameters for the entire polarizer, as shown in Fig. 3(c).

III. Results

Figure 4(a) shows the computed propagation constants of the quasi- TE_{10} and quasi- TE_{01} modes in the loaded

waveguide versus frequency. The difference between the propagation constants, shown in Fig. 4(b), varies less than 1 percent between 11 GHz and 15.5 GHz. Running one adaptive pass on the HFSS software at 11.0 GHz and then sweeping over the entire frequency range seemed to give valid answers. The propagation constants calculated from the sweep varied a maximum of 0.01 percent from the propagation constants calculated from adaptive passes run at the endpoints.

In an empty waveguide, the eigenmodes on the surface of the input ports are independent of frequency; however, with the dielectric loading, this is no longer true [2]. Figure 5 shows the quasi- TE_{10} and quasi- TE_{01} eigenmodes at the ports for (a) a loaded waveguide at 6.0 GHz, (b) a loaded waveguide at 16.0 GHz, and (c) an unloaded waveguide. As the frequency increases, the modes in the loaded waveguide vary more from the TE_{10} and TE_{01} modes in an empty waveguide. At 16.0 GHz, sizable fields exist in the dielectric strips on the walls parallel to the fields of the empty waveguide modes.

With the eigenmodes dependent on frequency, some complications occur which the HFSS software does not handle well when a frequency sweep is performed. The eigenmodes are computed at each frequency and then ordered according to the propagation constants. The quasi- TE_{10} and quasi- TE_{01} eigenmodes in the loaded waveguide are ordered as the first and second modes at 9.5 GHz, but then are ordered as the first and third modes from somewhere around 10 GHz and above. When analyzing the interface section, three modes were used to ensure that both the modes of interest were always included. The HFSS only plots the eigenmodes for the last frequency computed, so the user does not necessarily know what the mode ordering is at lower frequencies in the sweep. Also, HFSS will not compute impedances unless the user has defined impedance lines on the ports. The impedance lines are the lines connecting the points of maximum voltage difference on the ports, and are different for each mode. Only one set of impedance lines may be defined for all the frequencies in a sweep, and they must be defined in the same order as the corresponding modes. When the modes are switched during a sweep, the impedance lines are no longer valid at every frequency, and impedances will not be computed for any modes at any frequencies.

The S-parameters for the interface section between a 0.01-in. long slice of unloaded waveguide and a 0.1-in. long slice of loaded waveguide are plotted in Fig. 6. These S-parameters were used to construct the S-parameters for an entire polarizer of length 4.73 in. The S-parameters and differential phase shift for this polarizer are shown in

Fig. 7. The magnitude of the S_{11} parameter is large, indicating a poor impedance match at the interface. Also, the differential phase shift is not very constant, which also may be caused by a poor impedance match at the interface. To correct these problems, an input-matching section needs to be designed.

In an initial attempt to design an input-matching section, the impedances given by HFSS were examined. HFSS computes the impedance three ways. The first impedance, Z_{pi} , is derived from the input power and current calculated in the field solution. The second impedance, Z_{pv} , is computed from the input power from the field solution and the voltage across the impedance line on the port (the impedance line is defined by the user). The third impedance, Z_{vi} , is the geometric mean of the other two. These three impedances should be the same except for a multiplying constant; however, this was not the case. The three impedances, normalized to the 9.5-GHz values, are compared in Fig. 8.

IV. Conclusions

The results shown in Fig. 4 indicate that the polarizer design will function over a wide band. However, the return loss of the polarizer is quite high, and the differential phase shift is not as constant as desired. An input-matching section needs to be designed to correct both of these problems. The impedances as calculated by HFSS seem to be inconsistent. The values for S-parameters and impedances given by HFSS need to be compared with actual measurements on a polarizer to verify the results.

The HFSS software on the Sun SPARC 1+ workstation runs too slowly and uses too much hard-disk memory to handle large problems. As the number of modes, the size of the structure, and the complexity of the structure increase, HFSS rapidly slows down and uses more memory. Whenever possible, the problem needs to be broken down into smaller, more manageable pieces which can be recombined after analysis with HFSS.

References

- [1] E. Lier and T. Schaug-Pettersen, "A Novel Type of Waveguide Polarizer with Large Cross-Polar Bandwidth," *IEEE Transactions on Microwave Theory and Techniques*, vol. 36, pp. 1531–1534, November 1988.
- [2] R. F. Harrington, *Time Harmonic Electromagnetic Fields*, New York: McGraw-Hill, pp. 158–163, 1961.

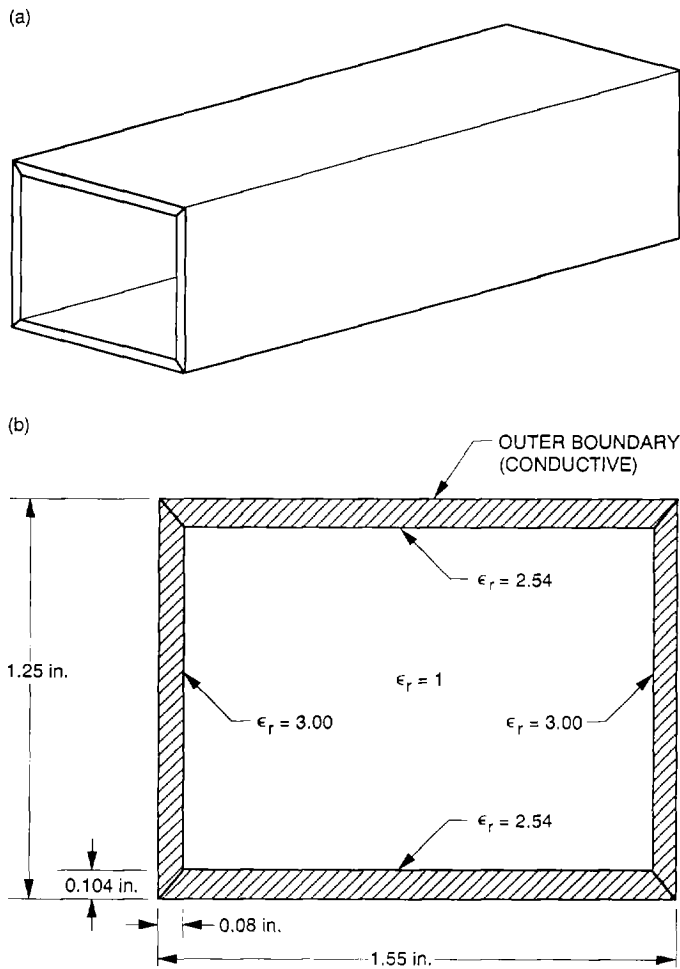


Fig. 1. Geometry of the polarizer: (a) polarizer and (b) cross-section.

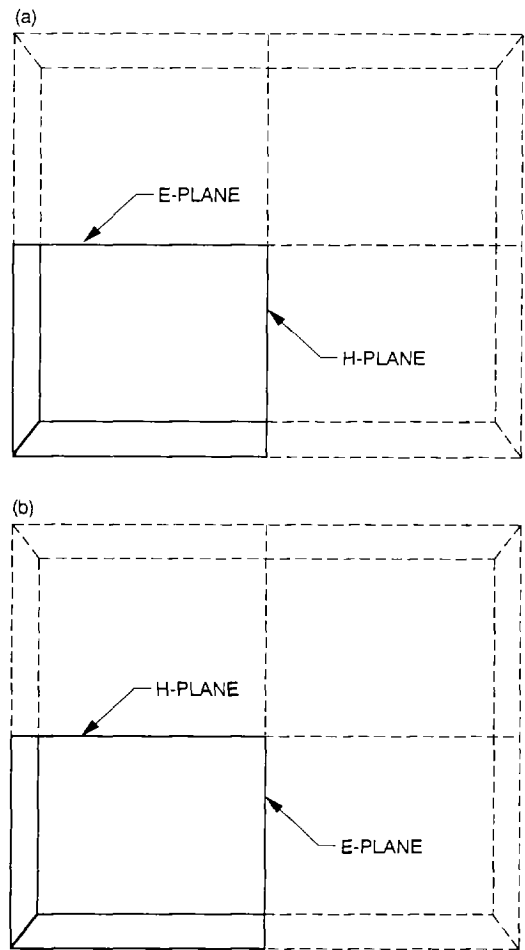


Fig. 2. Placement of planes of symmetry: (a) to analyze mode resulting from a TE_{10} mode input; and (b) to analyze mode resulting from a TE_{01} mode input.

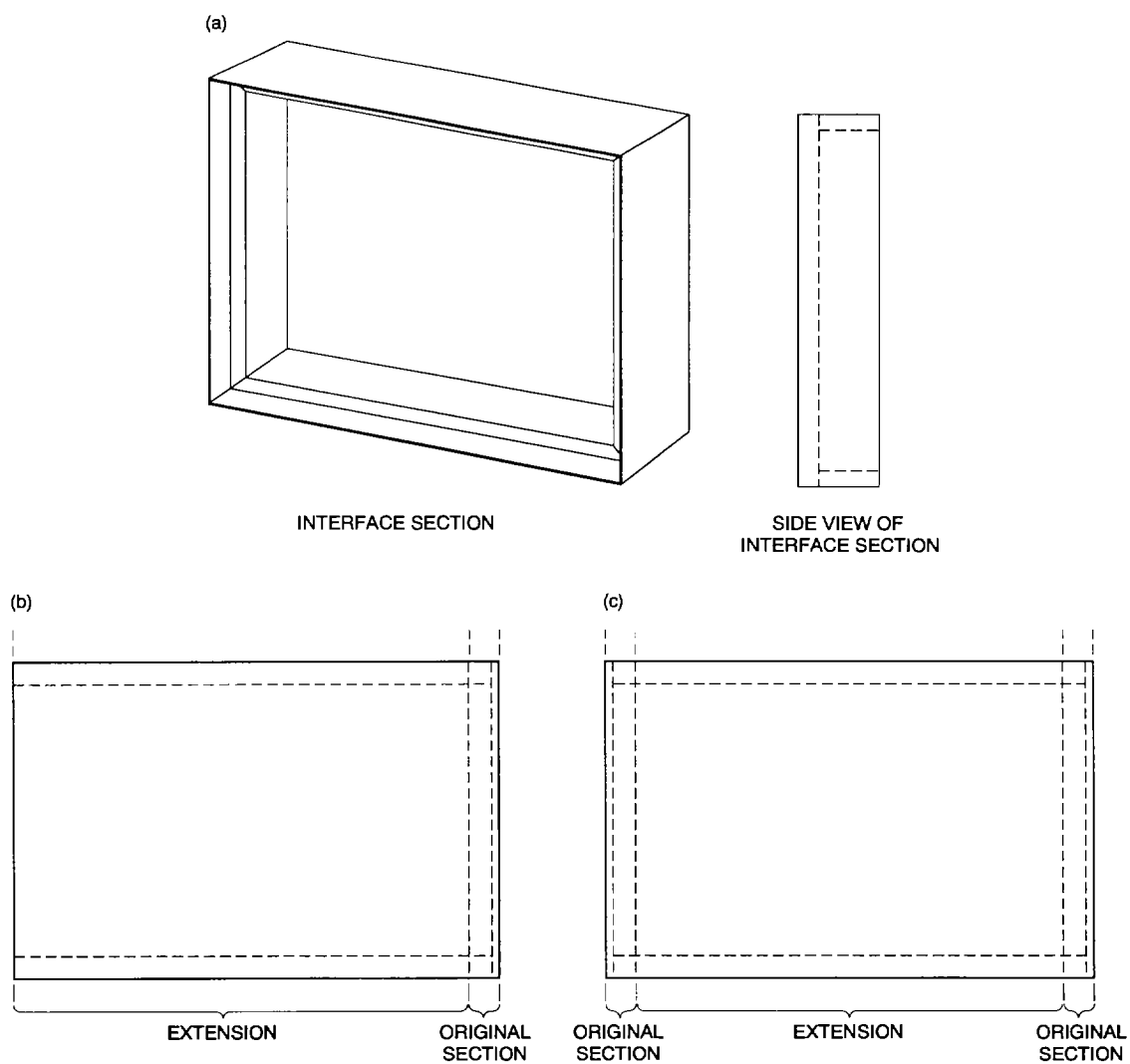


Fig. 3. Stages of polarizer analysis: (a) Interface section consisting of a thin slice of the loaded waveguide and a thin slice of empty waveguide; (b) side view of original section with extension; and (c) side view of total polarizer.

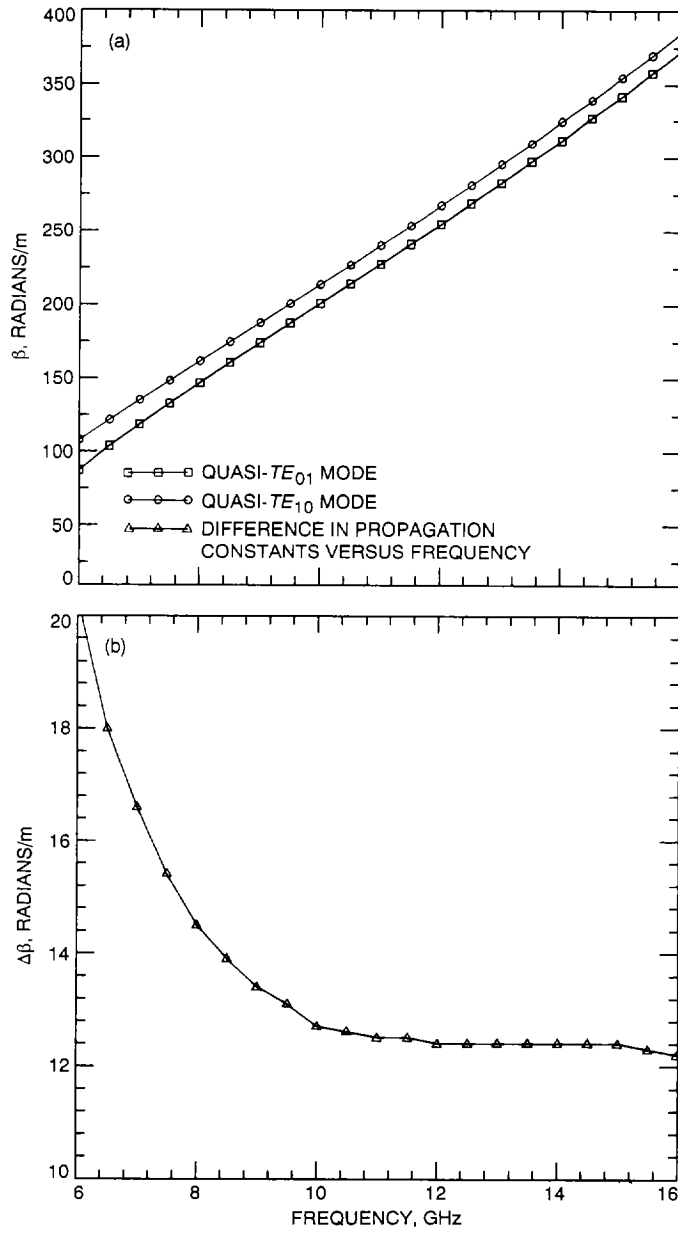


Fig. 4. Propagation constants of quasi- TE_{10} and quasi- TE_{01} modes: (a) β versus frequency and (b) $\Delta\beta$ versus frequency.

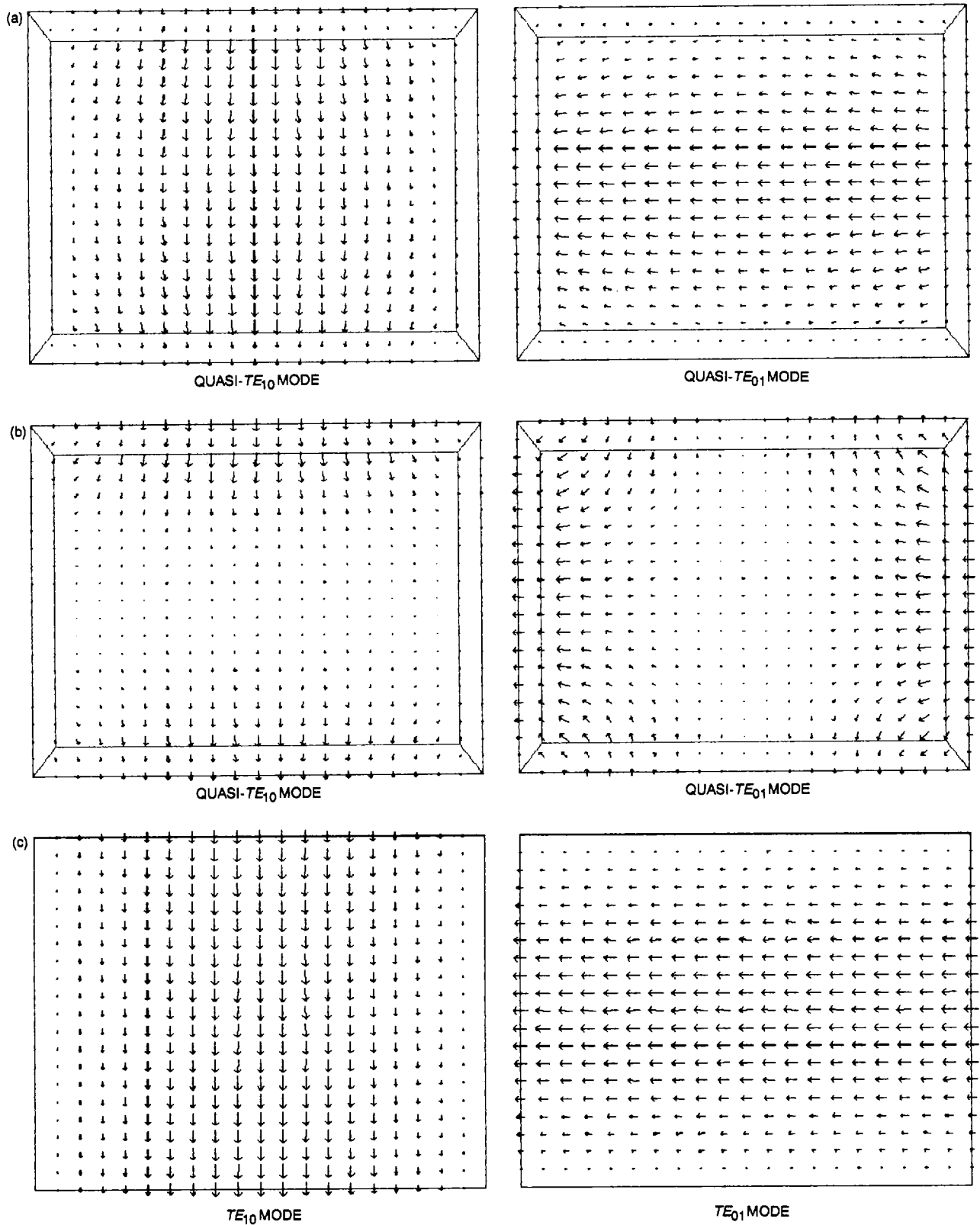


Fig. 5. Eigenmodes of interest at ports for (a) a loaded waveguide at 6.0 GHz; (b) a loaded waveguide at 16.0 GHz; and (c) an unloaded waveguide.

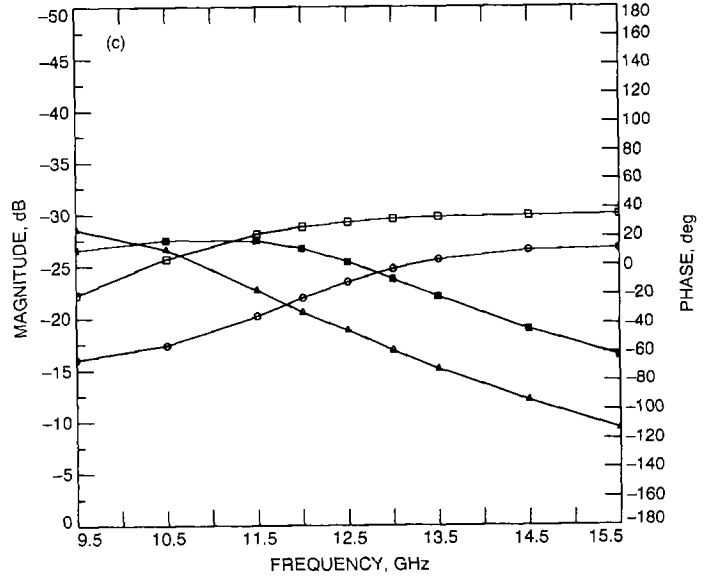
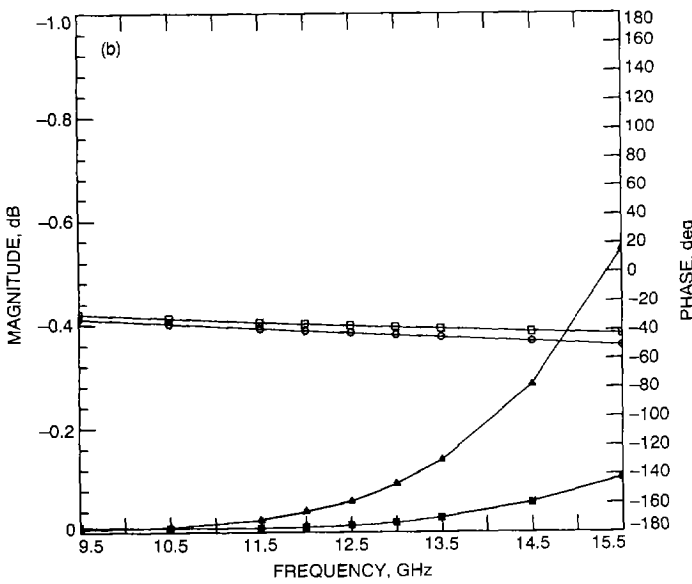
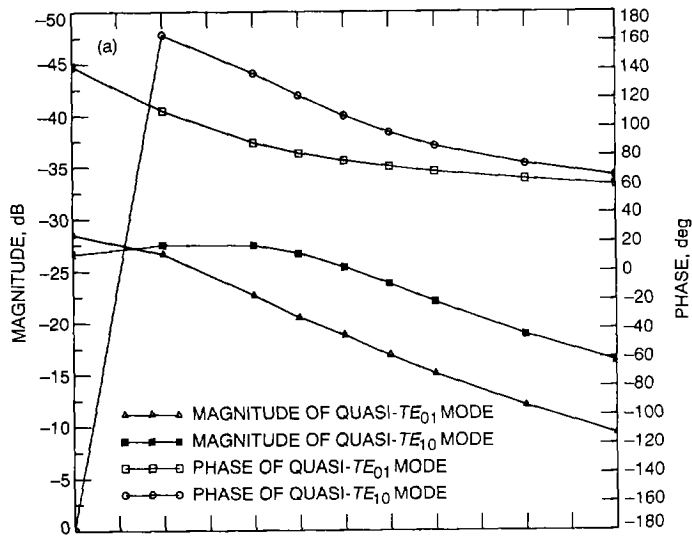


Fig. 6. S-parameters for interface section: (a) S_{11} ; (b) S_{12} ($= S_{21}$); and (c) S_{22} .

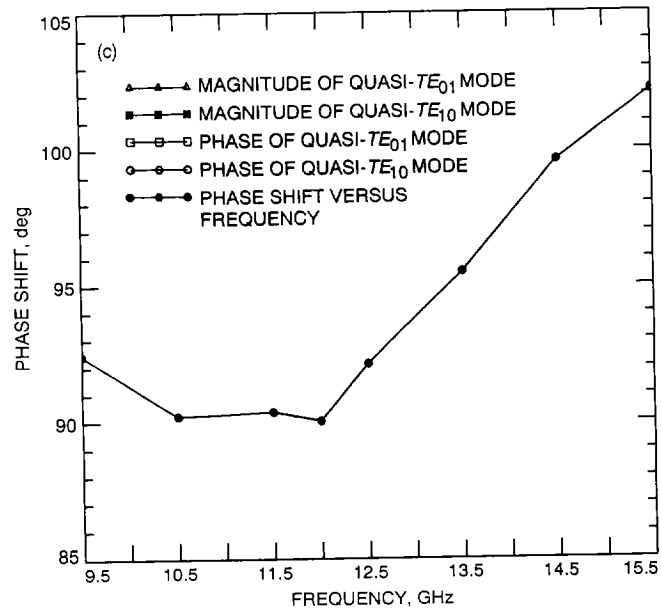
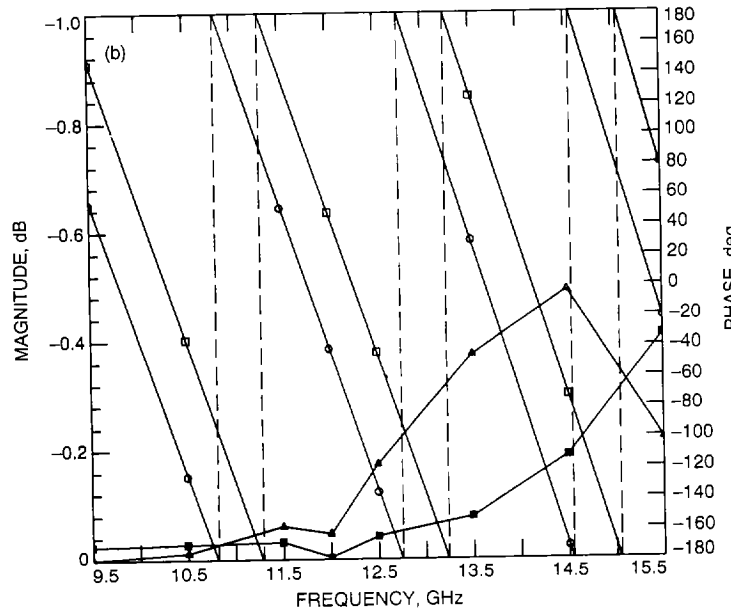
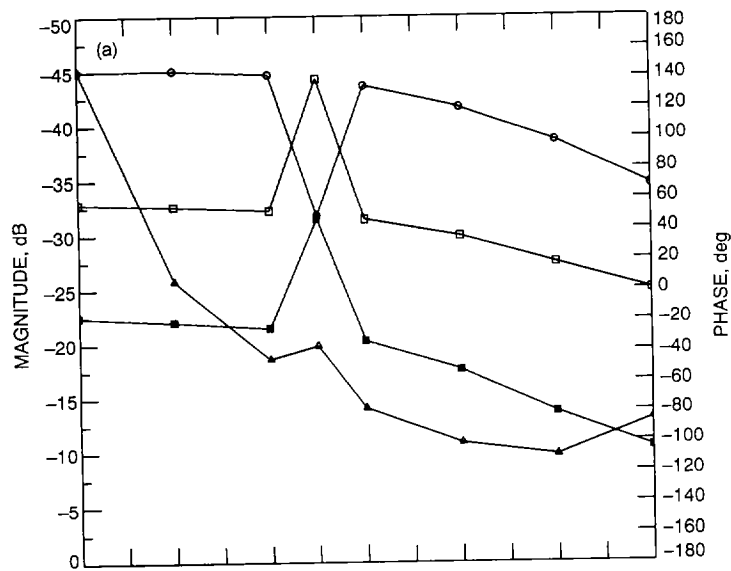


Fig. 7. Polarizer data: (a) S_{11} parameter; (b) S_{12} parameter; and (c) phase shift.

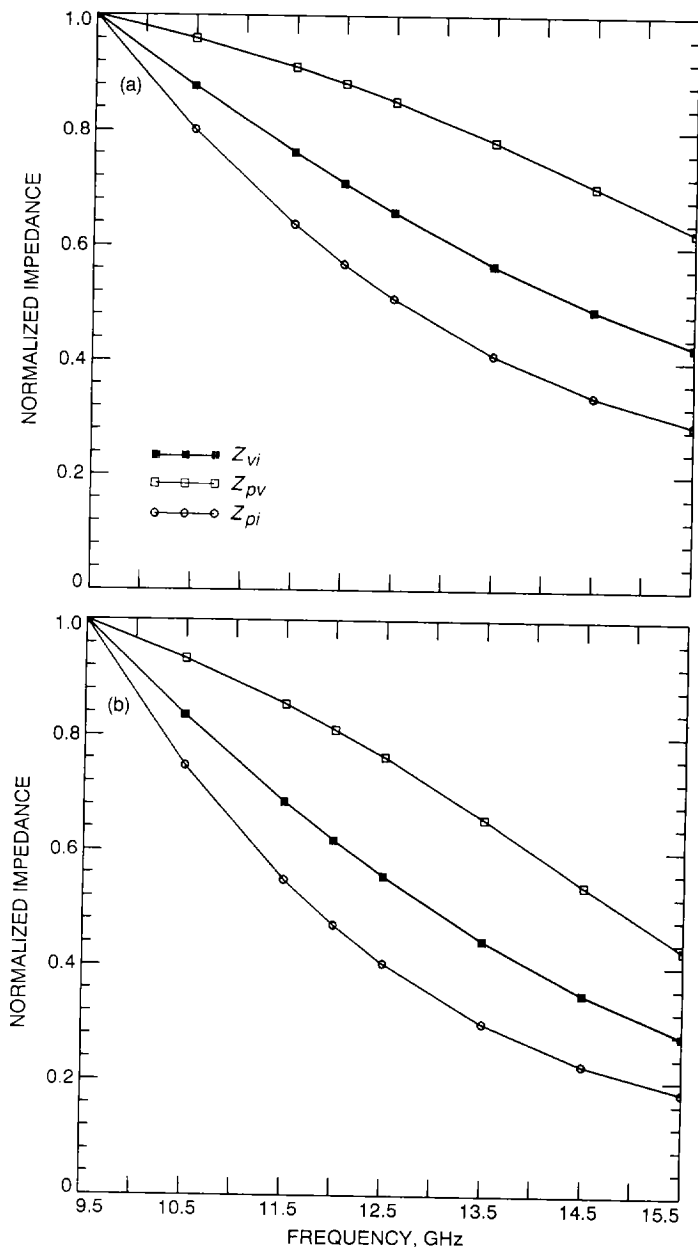


Fig. 8. Normalized impedances for (a) quasi- TE_{10} mode and (b) quasi- TE_{01} mode.